Hindawi
Advances in Materials Science and Engineering
Volume 2017, Article ID 4926543, 6 pages
https://doi.org/10.1155/2017/4926543

Research Article

Effect of Argon-Oxygen Mixing Gas during Magnetron Sputtering on TiO_2 Coatings

N. Madaoui,[1] L. Bait,[1] K. Kheyar,[2] and N. Saoula[1]

[1] *Division Milieux Ionisés et Lasers, Centre de Développement des Technologies Avancées (CDTA), Cité du 20 Août 1956, Baba Hassen, BP no. 17, Alger, Algeria*
[2] *Faculté de Physique Université Des Sciences et de la Technologie Houari Boumediene, BP 32, El Alia, Bab Ezzouar, 16111 Alger, Algeria*

Correspondence should be addressed to N. Saoula; nsaoula@yahoo.fr

Received 1 February 2017; Accepted 29 May 2017; Published 22 June 2017

Academic Editor: Fernando Lusquiños

A reactive r.f magnetron sputtering method was used to deposit titanium dioxide coating on stainless steel substrates without intentional heating or biasing. The purpose of this work is given to study the argon-oxygen mixing gas on the corrosion behavior of TiO_2 coatings. The morphology and structure of the coatings were studied by X-ray diffraction (XRD). Potentiodynamic polarization was used to study the corrosion behavior of the coatings. The results obtained from potentiodynamic polarization curves showed that TiO_2 coatings possessed higher corrosion resistance than uncoated substrate.

1. Introduction

Over the last few years, a great attention has been focused on the titania. TiO_2 coatings are extensively used in a wide range of applications such as gas sensor, high refractive index, nontoxicity, good mechanical properties, and the photocatalysts due to remarkable optical, electrical, and chemical properties [1–4]. Coatings such as TiO_2, SiO_2, and Al_2O_3 with very low electronic conductance or insulating properties are known to effectively protect metals and alloys from corrosive environment. Titanium dioxide (TiO_2) exhibits wide band gap and possesses good passivating surface with low anodic dissolution rate making it one of the promising materials for corrosion protection [5–7]. Different deposition techniques, such as chemical vapor deposition [8], dip coating [9], magnetron sputtering [10], are used to deposit TiO_2 coatings.

The objective of this study is to reveal the effects of oxygen partial pressure on the corrosion behavior properties of the TiO_2 thin coating, deposited on unheated substrates by modifying the O_2 concentration in Ar/O_2 mixture of an r.f. magnetron sputtering discharge under two distinct sputtering powers.

2. Materials and Methods

2.1. Deposition of TiO_2 Coating. TiO_2 coatings were deposited by r.f. (13.56 MHz) magnetron sputtering onto stainless steel substrates (1 cm in diameter). The details of the deposition chamber can be found in our previous work [11, 12]. The distance between the target and the substrate holder is about 55 mm. The gases used are high-purity argon (99.99990%) as the working gas and oxygen (99.99%) as reactive gas. After evacuating the sputtering chamber down to a pressure of 1.33×10^{-7} Pa, the gases ($Ar + O_2$) were introduced into the chamber.

The TiO_2 thin films were deposited onto steel (cylindrical: thickness and diameter of 1 cm), where their working faces were mechanically polished to a mean roughness of about 20 nm. Thereafter the samples were ultrasonically cleaned in an acetone bath for 10 min, followed by rinsing with alcohol and then air dried prior to the deposition process. In our previous work [12, 13], we showed that the physical and chemical properties of TiO_2 films are strongly influenced by the value of applied negative bias on the substrate in the magnetron sputtering. In the present work, we limit our

Table 1: Sputtering conditions for the deposition of TiO_2 coatings.

Target	Pure Ti metal (Φ76 × 5 mm) (99.95%)
Substrate	Stainless steel
Target-substrate distance	3 cm
Sputtering gas	Ar
Reactive sputtering gas	O_2
Flux rate of oxygen	5, 10, 20, and 30%
Sputtering gas pressure	30 mTorr
Bias substrate	−20 V
Deposition time	60 min
Power sputtering	200 W
Substrate temperature	Not heated

investigation to the effect of oxygen partial pressure on the TiO_2 films deposited by magnetron sputtering, while keeping the rest of the parameters constant (see Table 1). In order to improve the adhesion of the TiO_2 on steel an intermediate layer of Ti of 200 mm thickness was deposited [14, 15] which enhances the nucleation density and reduces the surface roughness of the coating.

2.2. Characterization. To investigate the structure of TiO_2 films deposited on the stainless steel surface, a Bruker Axe D8 Advance diffractometer was used in a Bragg-Brentano geometry, at room temperature, with Cuα K radiation (Kα = 1.5406 Å). The diffractometer acquiring range is between 0 and 90°, with a 0.01° resolution and the angle of incidence minimum is 0.1°. The mechanical properties of the films, such as hardness (H) and Young's modulus (E), were investigated using the CSM Instrument Switzerland nanoindenter equipped with a Berkovich diamond indenter tip. In order to avoid the effect of nonuniformity of the coating, a series of 10 indents were performed and the results were averaged. The indenter was operated in the continuous stiffness mode with a maximum load of 100 mN. The applied load is 3 mN. The indents were separated by about 10 μm for preventing overlapping effects. Fourier transform infrared (FTIR) analysis has been done in reflection mode in the setting (70, polarized light) with wavenumbers in the range 4000–400 cm^{-1} using a (Thermo Nicolet Nexus) spectrometer equipped with a deuterated triglycine sulphate detector.

The corrosion resistance of TiO_2 coatings was evaluated by potentiodynamic polarization test using a PARSTAT 4000. The measurement was conducted using a conventional three-electrode electrochemical cell in 3.5 wt. % NaCl solution: a saturated calomel electrode (SCE) as the reference electrode, a carbon as the counter electrode (CE), and the samples with 1 cm^2 exposed area as the working electrode (WE).

3. Results and Discussion

3.1. Structure. Commonly, TiO_2 is found in two stable crystalline phases, anatase and rutile, when it is deposited by reactive magnetron sputtering. The phase composition of the TiO_2 films is shown in Figure 1. The patterns show that the deposited films exhibit a crystalline phase and the strong

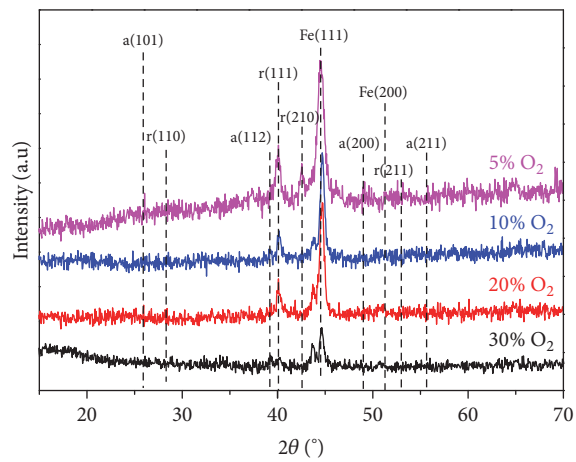

Figure 1: XRD diffraction patterns of TiO_2 films obtained for different oxygen flow rate (a: anatase, r: rutile, and Fe: iron).

peak observed at $2\theta = 45°$ corresponds to (111) plane of iron generated by the substrate. The crystalline structure of TiO_2 films changes from pure rutile (percentage of O_2 = 30%) to the mixture of anatase and rutile with decreasing content of oxygen in argon-oxygen gas mixture (percentage of O_2 = 20, 10 and 5%). The patterns show that the obtained films are crystalline and exhibited diffraction peaks at 27.5°, 41.3°, 44.1°, and 54.4°, corresponding, respectively, to (110), (111), (210), and (211) planes of rutile TiO_2 phase. The planes of anatase (101), (112), (200), and (211) are localized at 25.3°, 38.6°, 48.1°, and 55.1°, respectively. Safeen et al. [16] and Majeed et al. [17] found that the TiO_2 films have grown in amorphous phase. This is attributed to low-surface mobility of deposition particles, and hence, the deposition particles do not possess enough energy to crystallize [18]. Safeen et al. found a semicrystalline phase at higher substrate temperatures (⩾300°C) [16]. Majeed et al. [17] found that when a negative bias is applied to the substrate, it can lead to an increase in the energy of the surface atoms resulting in an enhanced surface diffusion, which can cause better adhesion, nucleation, and crystal structure. When the substrate is biased, more energy is transferred from ions driven by the substrate bias to the growing film, which can make the film more compact [19]. Nevertheless, in this work, the substrate was not heated but was biased at −20 V, enough to make the film crystallized (Figure 1).

Highest diffraction peak intensity indicates that rutile (111) is the preferential orientation from the broadening of diffraction peaks; the grain size was estimated using the Scherrer formula [20]: $D = (K \cdot \lambda)/\beta \cos\theta$, where $K = 0.89$, λ is the wavelength of X-ray, θ is the diffraction angle, and β is the corrected half width. The grain size of the TiO_2 thin films decreases from 16.2 to 6.7 nm as the oxygen flow rate decreases from 30 to 5% (Table 2). These results corresponded to the result of Safeen et al. [16] who deposited TiO_2 films by radio-frequency magnetron sputtering, and they found that the grain size of the film prepared in 10% O_2 was smaller than the film grown in 20% O_2. Also, similar result was reported by Zhao et al. [21] and Dannenberg and Greene [22]; they

Table 2: Grain size of rutile with (111) orientation at different O_2 flow rate.

O_2 (%)	Pos. (2θ)	FWHM (°)	D (nm)
30	40.14	0.091	16.2
20	40.14	0.120	12.3
10	40.10	0.112	13.2
5	40.10	0.221	6.7

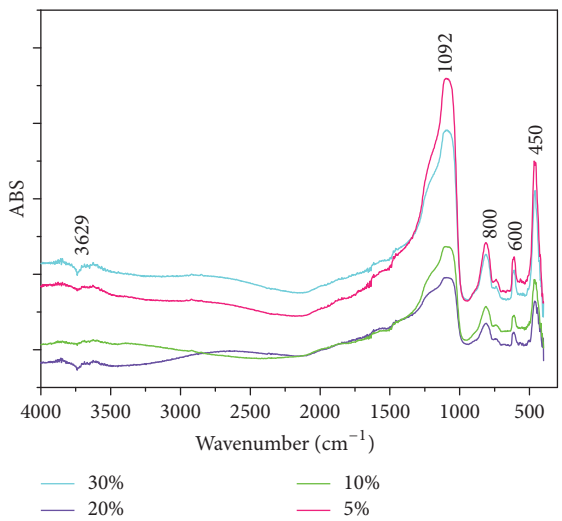

Figure 2: FTIR spectra of TiO_2 under different flow rate of oxygen.

related this results to the oxygen atoms which are reflected from the target and hit the substrate with appreciable energy, thereby causing nucleation [21, 22]. However, Zhao et al. [21] have noticed that too much oxygen will decrease the presence of Ti atoms in the vapor phase, thereby hindering nucleation and the films become amorphous.

3.2. FTIR Spectra. Figure 2 shows the Fourier transform infrared (FTIR) spectra of the TiO_2 coatings deposited under different flux rate of oxygen in range of 4000–400 cm^{-1}. According to Chandra Sekhar et al. [23], the presence of absorption bands indicates that the TiO_2 are crystalline for all conditions. It can be seen that the coatings exhibited broad and strong absorption peaks located in the range of 400 to 1000 cm^{-1}, which corresponded to stretching vibration of Ti-O and Ti-O-Ti bonds [13, 24–27]. The strong absorption bands at 1092 cm^{-1} are attributed to the vibration of stretching and deformation of Si-O-Si bond stemming from the glass substrate [23].

3.3. Mechanical Properties. Figure 3 gives the variation of the hardness (Hi) and elastic modulus (Ei) values of TiO_2 coatings. The results were given in Figure 5. The application of a negative bias to the substrate leads to an increase of the hardness and the elastic modulus. The maximum hardness and Young's modulus of $H = 11.3$ GPa and $E = 84.3$ GPa are obtained for a coating deposited under lower flux rate of oxygen. When the rate of oxygen increases the hardness

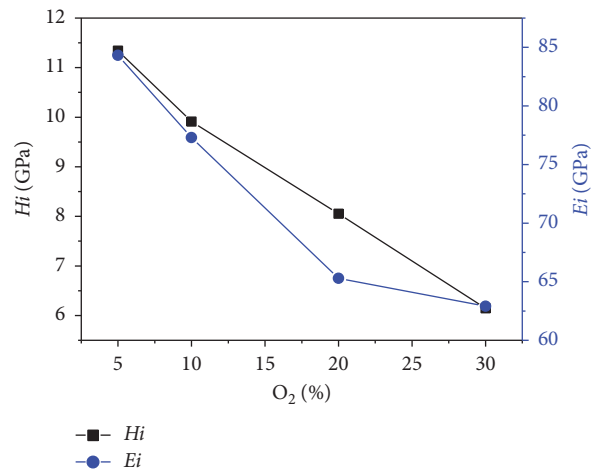

Figure 3: Hardness and Young's modulus of TiO_2 versus flux rate of oxygen.

decreases to lowest hardness of 6 GPa and lowest Young's modulus of 62 GPa. This result could be related to the same evolution of the grain size. Two other parameters are commonly used to evaluate the resistance to contact damage; they are expressed by two ratios: H/E and H^3/E^2 [28, 29]. The higher ratios of H/E or H^3/E^2 mean higher elastic and high resistance of coatings to plastic deformation and hence a higher wear resistance with low rigidity. The H/E is an indicator of film durability and is related to the elastic strain to failure capability (and resilience) in a surface contact, which is clearly important for the avoidance of wear [30]. The ratio H^3/E^2 is commonly used to evaluate the resistance to plastic deformation during wear or abrasion [28, 30].

Figure 4 shows the ratios H/E and H^3/E^2 for the various TiO_2 deposited under different flux rate of oxygen. It shows that all of the TiO_2 films present higher H^3/E^2, which indicates that TiO_2 films were characterized by good resistance to plastic deformation due to $H^3/E^2 > 0.1$ [30]. It is clear that the largest resistance to plastic deformation (i.e., maximum H/E and H^3/E^2) of values 0.13 and 0.2 GPa is found for sample deposited under lower flux rate of oxygen (5% O_2).

3.4. Electrochemical Polarization Analyses. Before each polarization test, the samples were immersed in aerated NaCl 3.5% at 25°C for a period of time for the OCP to stabilize. Figure 5 clearly shows that the presence of TiO_2 coatings on the metal surface in NaCl solution shifts both the anodic and cathodic branches of the Tafel plots to lower values of current density. This suggests that the modified TiO_2 coatings clearly retard the anodic dissolution process of stainless steel and increase its anticorrosion properties.

The electrochemical kinetic parameters in the polarization curves, such as the corrosion potential E_{corr}, corrosion current density i_{corr}, polarization resistance (Rp), corrosion rate (C_r), porosity (P), and the anodic and cathodic Tafel slopes (βa and βc) are listed in Table 1. It reveals from Table 3 that the corrosion current density i_{corr} was reduced

Table 3: Electrochemical parameters obtained from the Tafel method for stainless steel with and without coating of TiO_2 (in the operative conditions of the flow of oxygen) in 3.5% NaCl at 25°C.

Sample	E_{corr} (mV)	I_{corr} (nA·cm^{-2})	Rp (MΩ·cm^{-2})	C_r (mm/year)	Porosity (%)	Pe (%)
Stainless steel	−615.183	60709	0.000336301	35.01	1,091967969	—
30%	−134.679	16.328	7.83	0.0038309	9,128E − 06	99,97
20%	−188.135	17.69	5.777	0.0051917	8,03282E − 06	99,97
10%	−127.399	7.823	12.566	0.0017132	2,83173E − 06	99,98
5%	**−187.274**	**5.247**	**17.508**	**0.00093696**	**1,02758E − 08**	99,99

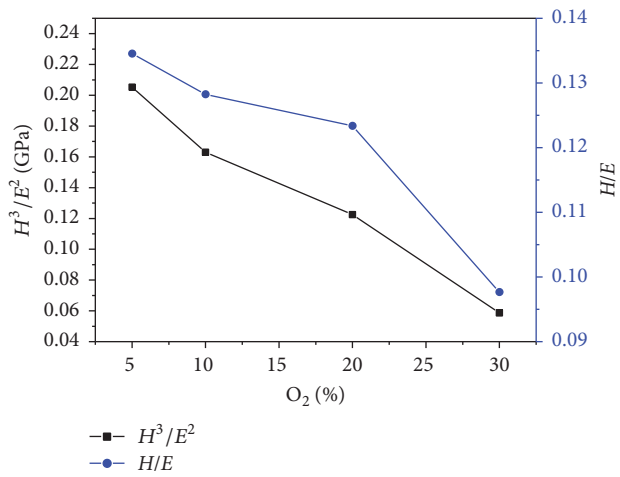

Figure 4: Variation of H/E and H^3/E^2 versus flux rate of oxygen.

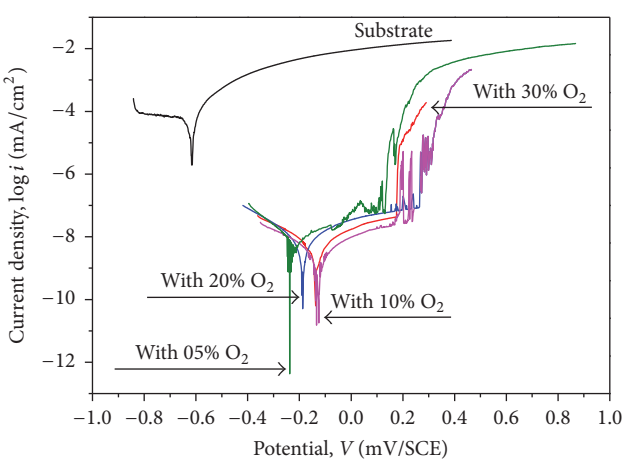

Figure 5: Effect of oxygen flow on the polarization curves of the stainless steel coated and uncoated in 3.5% NaCl solution, obtained at 25°C.

in the presence of TiO_2. Additionally, as shown in Table 3, E_{corr} values in the presence of the TiO_2 coatings were less negative than that in the absence of the TiO_2 coatings. On the other hand, the slight shifts of E_{corr} values towards positive direction are found with the increase of oxygen partial pressure O_2.

The pitting corrosion which occurs mainly depends on the concentration of Cl ions on the electrode surface. When the coatings are immersed in the solution rich in Cl ions, Cl ions absorb and concentrate on the surfaces of the specimens. The metal is dissolved into the solute because of the replacement of oxygen ions in the oxides of the coating by Cl ions. This condition induces the pitting. With the process of pitting reactions, a microgalvanic cell is gradually formed between the bared substrate in the pitting spot and the coating around the pitting spot, in which the former and the latter can be regarded as the anode and the cathode, respectively. This process will further accelerate the concentration of Cl ions in the pitting spot [31]. Dense coating provides very low permeability for electrolytes to establish an ionic conduct. The decrease in current density can be ascribed to the compact surface structure [32] and improved adhesion after decrease in oxygen partial pressure; at a lower oxygen flow rate, the nature of the substrate and oxygen flow can be an important factor influencing the quality of the coating [33], thereby reducing solution penetration and consequent localized corrosion. According to the corrosion surface, it was concluded that, after immersion for a period, the failure of the coatings could be ascribed to the micropores in the surface of coatings [34].

In our work, the current density of TiO_2 in 3.5% NaCl solution is (5.247 nA·cm^{-2}) much lower than both values obtained for nearly the same electrochemical conditions [35, 36], deposited by atomic layer deposition. Supplementary, the coating's protective efficiency (Pe) was determined from the polarization curve using the following equation:

$\mathrm{Pe} = [1 - (i_{corr,film}/i_{corr,substrate})] \times 100$, where $i_{corr,film}$ and $i_{corr,substrate}$ are the corrosion current densities of the coating and substrate in that order [12]. The results show that all the films work as corrosion protective coatings on stainless steel and each coating gives protection efficiency near or greater than 99% for all conditions. This result could be related to the grain size (Table 2); the film exhibiting the lowest grain size gives a high protective efficiency and a good hardness.

4. Conclusion

TiO_2 coatings have been successfully deposited on steel substrates by rf reactive magnetron sputtering a metallic target of titanium in an argon/oxygen atmosphere without heating. The X-ray diffraction results show that the coatings are crystalline. These coatings improve the corrosion resistance of stainless steel in NaCl solution with 3.5% Wt, but the protective properties of the coatings depend on the oxygen partial pressure. A TiO_2 coating with lower oxygen partial pressure showed the best protective properties. The best corrosion resistance was found for stainless steel at 5%

of oxygen partial pressure. The effective protection against corrosion is near 99% for all samples.

Conflicts of Interest

The authors declare that they have no conflicts of interest.

Acknowledgments

This research was financially supported by Grant of the National Funding of Research (FNR) (Ministère de l'Enseignement Supérieur de la Recherche Scientifique, Algérie).

References

[1] C. Zhang, W. Ding, H. Wang, W. Chai, and D. Ju, "Influences of working pressure on properties for TiO_2 films deposited by DC pulse magnetron sputtering," *Journal of Environmental Sciences*, vol. 21, no. 6, pp. 741–744, 2009.

[2] B. S. Richards, "Single-material TiO_2 double-layer antireflection coatings," *Solar Energy Materials and Solar Cells*, vol. 79, no. 3, pp. 369–390, 2003.

[3] J. Yu and X. Zhao, "Effect of substrates on the photocatalytic activity of nanometer TiO_2 thin films," *Materials Research Bulletin*, vol. 35, no. 8, pp. 1293–1301, 2000.

[4] B. Karunagaran, P. Uthirakumar, S. J. Chung, S. Velumani, and E.-K. Suh, "TiO_2 thin film gas sensor for monitoring ammonia," *Materials Characterization*, vol. 58, no. 8-9, pp. 680–684, 2007.

[5] D. S. R. Krishna and Y. Sun, "Thermally oxidised rutile-TiO2 coating on stainless steel for tribological properties and corrosion resistance enhancement," *Applied Surface Science*, vol. 252, no. 1, 1107 pages, 2005.

[6] L. Bamoulid, M.-T. Maurette, D. de Caro et al., "An efficient protection of stainless steel against corrosion: combination of a conversion layer and titanium dioxide deposit," *Surface and Coatings Technology*, vol. 202, no. 20, 5020 pages, 2008.

[7] H. Yun, J. Li, H.-B. Chen, and C.-J. Lin, "A study on the N-, S- and Cl-modified nano-TiO_2 coatings for corrosion protection of stainless steel," *Electrochimica Acta*, vol. 52, no. 24, pp. 6679–6685, 2007.

[8] B. Vallejo, M. Gonzalez-Mañas, J. Martínez-López, F. Morales, and M. A. Caballero, "Characterization of TiO_2 deposited on textured silicon wafers by atmospheric pressure chemical vapour deposition," *Solar Energy Materials and Solar Cells*, vol. 86, no. 3, pp. 299–308, 2005.

[9] P. Dhivya, A. K. Prasad, and M. Sridharan, "Nanostructured TiO_2 films: Enhanced NH3 detection at room temperature," *Ceramics International*, vol. 40, Part A, no. 1, pp. 409–415, 2014.

[10] M. C. Liao, H. Niu, and G. S. Chen, "Effect of sputtering pressure and post-annealing on hydrophilicity of TiO_2 thin films deposited by reactive magnetron sputtering," *Thin Solid Films*, vol. 518, no. 24, pp. 7258–7262, 2010.

[11] N. Saoula, K. Henda, and R. Kesri, "Deposition of titanium nitride thin films onto silicon by rf reactive magnetron sputtering," *Materials Science Forum*, vol. 609, pp. 117–121, 2009.

[12] L. Bait, L. Azzouz, N. Madaoui, and N. Saoula, "Influence of substrate bias voltage on the properties of TiO_2 deposited by radio-frequency magnetron sputtering on 304L for biomaterials applications," *Applied Surface Science*, vol. 395, pp. 72–77, 2017.

[13] S. Nezar, N. Saoula, S. Sali et al., "Properties of TiO2 thin films deposited by rf reactive magnetron sputtering on biased substrates," *Applied Surface Science*, vol. 395, pp. 172–179, 2017.

[14] N. Saoula, N. Madaoui, R. Tadjine, R. M. Erasmus, S. Shrivastava, and J. D. Comins, "Influence of substrate bias on the structure and properties of TiCN films deposited by radio-frequency magnetron sputtering," *Thin Solid Films*, vol. 616, pp. 521–529, 2016.

[15] N. Saoula, K. Henda, R. Kesri, S. Shrivastava, R. M. Erasmus, and J. D. Comins, "Effect of the plasma deposition parameters on the properties of Ti/TiC multilayers for hard coatings applications," *Acta Physica Polonica A*, vol. 121, no. 1, pp. 172–174, 2012.

[16] K. Safeen, V. Micheli, R. Bartali, G. Gottardi, and N. Laidani, "Low temperature growth study of nano-crystalline TiO_2 thin films deposited by RF sputtering," *Journal of Physics D: Applied Physics*, vol. 48, no. 29, Article ID 295201, 2015.

[17] A. Majeed, J. He, L. Jiao, X. Zhong, and Z. Sheng, "Surface properties and biocompatibility of nanostructured TiO2 film deposited by RF magnetron sputtering," *Nanoscale Research Letters*, vol. 10, no. 56, 2015.

[18] Y. Shen, H. Yu, J. Yao et al., "Investigation on properties of TiO2 thin films deposited at different oxygen pressures," *Optics and Laser Technology*, vol. 40, no. 3, pp. 550–554, 2008.

[19] P. K. Song, Y. Irie, and Y. Shigesato, "Crystallinity and photocatalytic activity of TiO_2 films deposited by reactive sputtering with radio frequency substrate bias," *Thin Solid Films*, vol. 496, no. 1, pp. 121–125, 2006.

[20] N. Martin, A. M. E. Santo, R. Sanjinés, and F. Lévy, "Energy distribution of ions bombarding TiO2 thin films during sputter deposition," *Surface and Coatings Technology*, vol. 138, no. 1, pp. 77–83, 2001.

[21] B.-X. Zhao, J.-C. Zhou, and L.-Y. Rong, "Microstructure and optical properties of TiO_2 thin films deposited at different oxygen flow rates," *Transactions of Nonferrous Metals Society of China (English Edition)*, vol. 20, no. 8, pp. 1429–1433, 2010.

[22] R. Dannenberg and P. Greene, "Reactive sputter deposition of titanium dioxide," *Thin Solid Films*, vol. 360, no. 1-2, pp. 122–127, 2000.

[23] M. Chandra Sekhar, P. Kondaiah, S. V. Jagadeesh Chandra, G. Mohan Rao, and S. Uthanna, "Effect of substrate bias voltage on the structure, electric and dielectric properties of TiO_2 thin films by DC magnetron sputtering," *Applied Surface Science*, vol. 258, no. 5, pp. 1789–1796, 2011.

[24] N. Wang, W. Fu, J. Zhang, X. Li, and Q. Fang, "Corrosion performance of waterborne epoxy coatings containing polyethylenimine treated mesoporous-TiO_2 nanoparticles on mild steel," *Progress in Organic Coatings*, vol. 89, pp. 114–122, 2015.

[25] B.-T. Liu and P.-S. Li, "Preparation and characterization of high-refractive-index polymer/inorganic hybrid films containing TiO_2 nanoparticles prepared by 4-aminobenzoic acid," *Surface and Coatings Technology*, vol. 231, pp. 301–306, 2013.

[26] T. C. Jagadale, S. P. Takale, R. S. Sonawane et al., "N-doped TiO_2 nanoparticle based visible light photocatalyst by modified peroxide sol-gel method," *The Journal of Physical Chemistry C*, vol. 112, no. 37, pp. 14595–14602, 2008.

[27] M. Karimi Sahnesarayi, H. Sarpoolaky, and S. Rastegari, "Effect of heat treatment temperature on the performance of nano-TiO_2 coating in protecting 316L stainless steel against corrosion under UV illumination and dark conditions," *Surface and Coatings Technology*, vol. 258, pp. 861–870, 2014.

[28] J. Musil, "Hard and superhard nanocomposite coatings," *Surface and Coatings Technology*, vol. 125, no. 1-3, pp. 322–330, 2000.

[29] A. Leyland and A. Matthews, "On the significance of the H/E ratio in wear control: a nanocomposite coating approach to optimised tribological behaviour," *Wear*, vol. 246, no. 1-2, pp. 1–11, 2000.

[30] J. Musil, R. Jílek, M. Meissner, T. Tölg, and R. Čerstvý, "Two-phase single layer Al-O-N nanocomposite films with enhanced resistance to cracking," *Surface and Coatings Technology*, vol. 206, no. 19-20, pp. 4230–4234, 2012.

[31] L. F. Hu, J. Li, Y. F. Tao, and Y. H. Lv, "Corrosion behaviors of TiNi/Ti_2Ni matrix coatings in the environment rich in Cl ions," *Surface and Coatings Technology*, vol. 311, pp. 295–306, 2017.

[32] D. Xie, H. Wang, R. Ganesan, Y. Leng, H. Sun, and N. Huang, "Fatigue durability and corrosion resistance of TiO_2 films on CoCrMo alloy under cyclic deformation," *Surface and Coatings Technology*, vol. 275, pp. 252–259, 2015.

[33] A. H. Chiou, C. G. Kuo, C. H. Huang, W. F. Wu, C. P. Chou, and C. Y. Hsu, "Influence of oxygen flow rate on photocatalytic TiO_2 films deposited by rf magnetron sputtering," *Journal of Materials Science: Materials in Electronics*, vol. 23, no. 2, pp. 589–594, 2012.

[34] T. Liu, F. Zhang, C. Xue, L. Li, and Y. Yin, "Structure stability and corrosion resistance of nano-TiO_2 coatings on aluminum in seawater by a vacuum dip-coating method," *Surface and Coatings Technology*, vol. 205, no. 7, pp. 2335–2339, 2010.

[35] M. Chandra Sekhar, P. Kondaiah, B. Radha Krishna, and S. Uthanna, "Effect of oxygen partial pressure on the electrical and optical properties of DC magnetron sputtered amorphous TiO_2 films," *Journal of Spectroscopy*, vol. 2013, Article ID 462734, 7 pages, 2013.

[36] C. X. Shan, X. Hou, and K.-L. Choy, "Corrosion resistance of TiO_2 films grown on stainless steel by atomic layer deposition," *Surface and Coatings Technology*, vol. 202, no. 11, pp. 2399–2402, 2008.